Available online at www.sciencedirect.com
SCIENCE DIRECT
Journal of Power Sources 154 (2006) 42–50
JOURNAL OF POWER SOURCES
www.elsevier.com/locate/jpowsour

Influence of composition and Cu impregnation method on the performance of $Cu/CeO_2/YSZ$ SOFC anodes

Sukwon Jung, Chun Lu, Hongpeng He, Kipyung Ahn, R.J. Gorte, J.M. Vohs *

Department of Chemical and Biomolecular Engineering, University of Pennsylvania, Philadelphia, PA, USA

Received 26 February 2005; received in revised form 5 April 2005; accepted 5 April 2005
Available online 13 June 2005

Abstract

In this study, we report on how different impregnation procedures affect the distribution and morphology of the Cu component in $Cu/CeO_2/YSZ$ (YSZ, yttria-stabilized zirconia) composite anodes and how this affects anode performance. Two different methods for Cu addition to the porous YSZ anode were investigated: impregnation using aqueous solutions of $Cu(NO_3)_2$ and impregnation using aqueous solutions of $Cu(NO_3)_2$ plus urea. The latter method produced a homogeneous distribution of Cu throughout the anode while the former resulted in a higher concentration of Cu near the exposed surface relative to that in the bulk. Studies of the thermal stability of the deposited copper layers and the influence of the Cu distribution on cell performance when operating with humidified H_2 as the fuel are also presented.

Keywords: Fuel cells; Ceria; Copper; Anodes

1. Introduction

In previous studies, we have reported on the use of wet impregnation methods for the fabrication of $Cu/CeO_2/YSZ$ (YSZ, yttria-stabilized zirconia) composite anodes for solid oxide fuel cells (SOFC) [1–8]. In this method of anode fabrication, a highly porous YSZ anode matrix is initially prepared by sintering a green YSZ tape which contains pyrolyzable pore formers, such as graphite. The electronic conductor, Cu, and an oxidation catalyst, CeO_2, are then added to the pores via impregnation with aqueous solutions of copper and cerium nitrates followed by oxidation to form CeO_2 and reduction to form Cu. The fact that these latter steps require temperatures below 750 K is one of the advantages that this approach has over more conventional anode fabrication techniques, since it allows materials, such as Cu, that melt at temperatures significantly less than sintering temperature required for the YSZ component, to be incorporated into the anode. The fact that high-temperature processing is not required for the impregnated components also allows deleterious reactions between the various components in the anode to be avoided. Thus, the method provides significant flexibility in terms of the anode composition and the optimization of catalytic and electronic properties. Indeed, the composition of the $Cu/CeO_2/YSZ$ composite anodes was chosen in order to allow for operation of SOFCs with hydrocarbon fuels without the need for first reforming the fuel into a hydrogen-rich synthesis gas and these anodes have been shown to exhibit good performance for this application [2–6,8,9].

While the wet impregnation method allows for tailoring of the anode composition for specific applications, optimization of the structure and morphology of the impregnated species are also important in order to obtain high performance. For example, in $Cu/CeO_2/YSZ$ anodes the copper component primarily provides a conduction path out of the anode for the electrons produced by oxidation of the fuel at the three-phase boundary between the anode and the electrolyte [2]. The copper deposits need to be well interconnected in order to provide this conduction path. Likewise, the ceria catalyst needs to be present at the three-phase boundary and ideally would have high surface area in order to maximize

* Corresponding author. Tel.: +1 215 898 6318; fax: +1 215 573 2093.
E-mail address: vohs@seas.upenn.edu (J.M. Vohs).

0378-7753/$ – see front matter © 2005 Elsevier B.V. All rights reserved.
doi:10.1016/j.jpowsour.2005.04.018

the number of sites where the fuel oxidation reaction can take place.

The goal of the present study was to investigate how the amount, morphology and spatial distribution of impregnated Cu and CeO_2 components influence the performance of Cu/CeO_2/YSZ anodes when operating with H_2 as the fuel. In order to control the spatial distribution and the morphology of the Cu deposits in the anode, two separate impregnation procedures were used: (1) impregnation with aqueous copper nitrate solutions and (2) impregnation with aqueous copper nitrate solutions containing urea. In the former method, the impregnated solutions are allowed to dry resulting in the formation of $Cu(NO_3)_2$ precipitates that are subsequently reduced to Cu metal via heating in H_2. In this case, the morphology of the initial copper deposits is controlled by the drying process as will be shown below this method does not produce a uniform distribution of Cu in the anode. In the latter method in which urea is included in the impregnation solution, the following reactions take place upon heating to ~350 K [10,11].

$$CO(NH_2)_2 + H_2O \rightarrow 2NH_4 + 2OH^- + CO_2\,(g) \quad (1)$$

$$Cu^{2+} + 2OH^- \rightarrow Cu(OH)_2\,(s) \quad (2)$$

Since these reactions occur prior to evaporation of the water solvent, the deposition of the $Cu(OH)_2$ occurs in a homogeneous manner and is not affected by the drying process. Thus, following reduction one would expect a more even distribution of Cu in the YSZ matrix when using solutions containing urea compared to those containing only the dissolved copper nitrate. As will be shown below, this is indeed the case. The effect of these changes in copper film morphology on anode performance is also discussed.

2. Experimental methods

The methods used to fabricate the fuel cells used in this study have previously been described in detail [1–4,7,8] and only a brief description is given here. The cells were constructed from discs with a dense YSZ electrolyte layer in contact with a porous YSZ anode layer. These bilayers discs were cut from green tapes produced by casting a YSZ (Tosoh 8 mol% Y_2O_3) layer containing graphite and polymethylmethacrylate (PMMA) pore formers onto a thin YSZ electrolyte layer. Following calcination in air at 1823 K for 4 h, the dense electrolyte layer was 45 μm in thickness and the anode layer was 300 μm in thickness with a porosity of ~65%. A 0.35 cm^2 cathode was applied by painting a slurry containing a 50:50 wt.% mixture of YSZ and $La_{0.8}Sr_{0.2}MnO_3$ (LSM, Praxair), and graphite pore formers onto the exposed surface of the YSZ electrolyte followed by calcination in air at 1673 K for 2 h.

Subsequent to the steps requiring high-temperature calcination, ceria and Cu salts were added to the anode using a series of wet impregnation steps. Ceria was initially added by impregnating with an aqueous ceria nitrate solution ($Ce(NO_3)_3$, AlfaAesar) followed by calcination in air at 723 K. Cu was then added to the porous YSZ anode matrix using either an aqueous solution of copper nitrate or an aqueous solution containing copper nitrate and urea ($CO(NH_2)_2$, AlfaAesar) in a 1:1.5 molar ratio. As described in Section 1, when using the copper nitrate/urea solution the copper ions and urea react forming copper hydroxide upon heating to 335 K [10,11]. In both cases, the deposited copper salts were converted to copper oxide by calcining in air at 723 K and were then reduced to Cu metal upon activation of the cell in flowing H_2. The loadings of both ceria and Cu in the anode were controlled by varying the amounts of impregnation solution used and the number of impregnation steps and are reported as volume percent of the anode. For example, to incorporate 13 vol% Cu into the porous YSZ matrix, ~12 successive impregnation steps were required for both the copper nitrate and copper nitrate/urea solutions and to achieve 5 vol% CeO_2, ~6 impregnation steps were required.

Ag and Au current collectors were attached to the cathode and anode sides of each cell, respectively. With one exception, the anode current collector consisted of a ring of Au wire that was approximately two-thirds the diameter of the cell that was attached along the entire length of the wire using an Au paste. For one cell, a gold mesh was used as the anode current collector. For performance testing, the cells were attached to an alumina tube using a ceramic adhesive and pre-treated by heating in humidified H_2 (3% H_2O) to 973 K and held for 2 h. All *V–I* (voltage–current) curves were measured at 973 K in humidified H_2 (3% H_2O) with a flow rate of 50 ml/min and impedance spectra were collected in the galvanostatic mode at a current density of 300 mA cm^{-2} using a Gamry Instruments Model EIS 300 impedance spectrometer.

In addition to tests using fuel cells, the microstructure and electronic properties of CeO_2 and Cu impregnated porous YSZ blocks were characterized using four-point conductivity measurements and scanning electron microscopy (SEM). These samples were produced by sintering pieces cut form a thick YSZ green tape containing pore formers followed by impregnation with CeO_2 and Cu using the methods described above.

3. Results and discussion

3.1. Conductivity measurements

As a base case for comparison, the electronic conductivity of porous YSZ blocks impregnated with either CeO_2 or Cu were initially measured as a function of the amount of impregnated species. These results are summarized in Table 1. The conductivity of each sample was measured at 973 K using the four probe method after being exposed to flowing H_2 at 973 K for 2 h. The conductivity of the ceria-impregnated samples increased a small amount with ceria loading, but as would be expected these samples all had very low conductiv-

Table 1
Conductivities of porous YSZ blocks impregnated with either CeO_2 or Cu using the nitrate-only method

Impregnated species	Vol%	Conductivity (S cm^{-1})
CeO_2	5	0.0079
	10	0.012
	15	0.019
Cu	5	0.0018
	10	251
	15	1190

ities. The conductivity of samples impregnated with Cu using the nitrate solution increased with metal loading and reached a value of 1190 S cm^{-1} for the sample containing 15 vol% Cu. This result is consistent with our previous studies [12]. Note that the relationship between conductivity and Cu content for the impregnated cermets is different from that of conventional Ni–YSZ [13] and Cu–YZT [14] cermets, where the metal is more randomly distributed and a sharp jump in conductivity is observed at a percolation threshold near 30 vol% metal. For the impregnated anodes, the Cu is deposited in the pores of a porous YSZ matrix and thus the metal is not randomly distributed and significant bulk conductivity is obtained at a much lower volume percent of metal.

In order to correlate with the properties of working anodes and study the effects of using urea when depositing Cu, conductivity measurements were also made for YSZ blocks impregnated with both Cu and CeO_2 using the nitrate and the nitrate/urea methods for the copper addition. The effect of annealing the impregnated samples in H_2 at temperatures up to 1173 K was also investigated. Results are presented in Table 2. Several trends are apparent in this data. First, adding more ceria produced an increase in the conductivity regardless of the method used to deposit the Cu, despite the fact that, as shown in Table 1, ceria does not impart any electronic conductivity. The likely explanation for this result is that since the ceria was added to the porous YSZ block prior to the Cu, it influences the distribution of the deposited Cu layer.

The most important result contained in the data in Table 2 is the effect of thermal treatment in H_2 on the overall electronic conductivity. For the samples impregnated with Cu using only copper nitrate solution, increasing the annealing temperature in H_2 from 973 to 1173 K caused the conductivity to decrease by ~12% regardless of the ceria loading. The samples impregnated with Cu using aqueous copper nitrate plus urea exhibited lower overall conductivities and a much more dramatic decrease in conductivity upon heating to 1173 K. For the 16/8 (Cu/CeO_2) and 16/12 samples, the decrease in conductivity upon increasing the annealing temperature in H_2 from 973 to 1173 K was 96 and 84%, respectively. These results suggest that there are significant differences in the distribution and/or morphology of the Cu films produced using only nitrate and nitrate/urea impregnation methods.

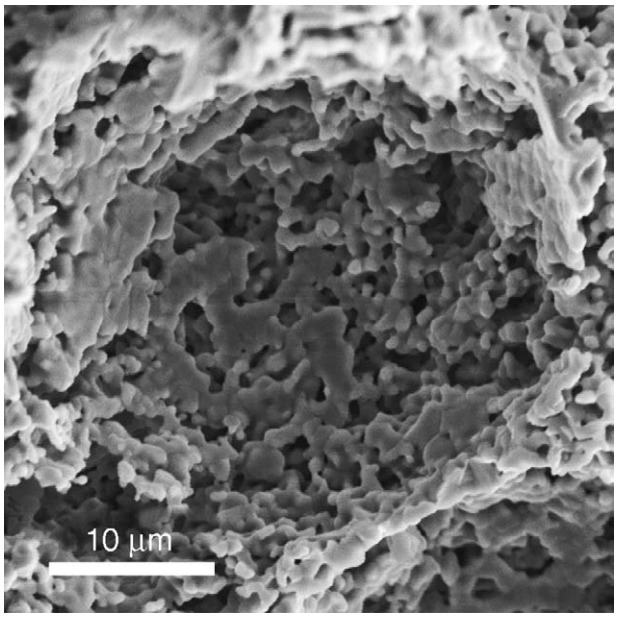

Fig. 1. SEM image of a porous YSZ block.

3.2. Microscopy

SEM was used to investigate the morphology of the Cu films produced using the two wet impregnation techniques. Fig. 1 displays an SEM image of the porous YSZ anode matrix prior to impregnation of ceria and copper. The large, spherical, ~40 μm pore shown in the image results from the pyrolysis of one of the PMMA beads which were used as pore formers, while the smaller micropores are due to pyrolysis of the graphite particles [1]. Fig. 2 shows SEM images of a large spherical pore near the center of the YSZ block after impregnation of ceria and copper, and reduction in H_2 for 2 h at 973 K. Copper was deposited without and with urea for the samples in Fig. 2A and B, respectively, and both samples

Table 2
Conductivity of YSZ blocks impregnated with Cu and CeO_2

Composition (vol%)	H_2 annealing temperature (K)	Block impregnated with Cu nitrate (S cm^{-1})	Block impregnated with Cu nitrate plus urea (S cm^{-1})
16% Cu, 8% ceria	700	678	300
	1073	605	81
	1173	596	12
16% Cu, 12% ceria	700	1002	950
	1073	896	477
	1173	892	155

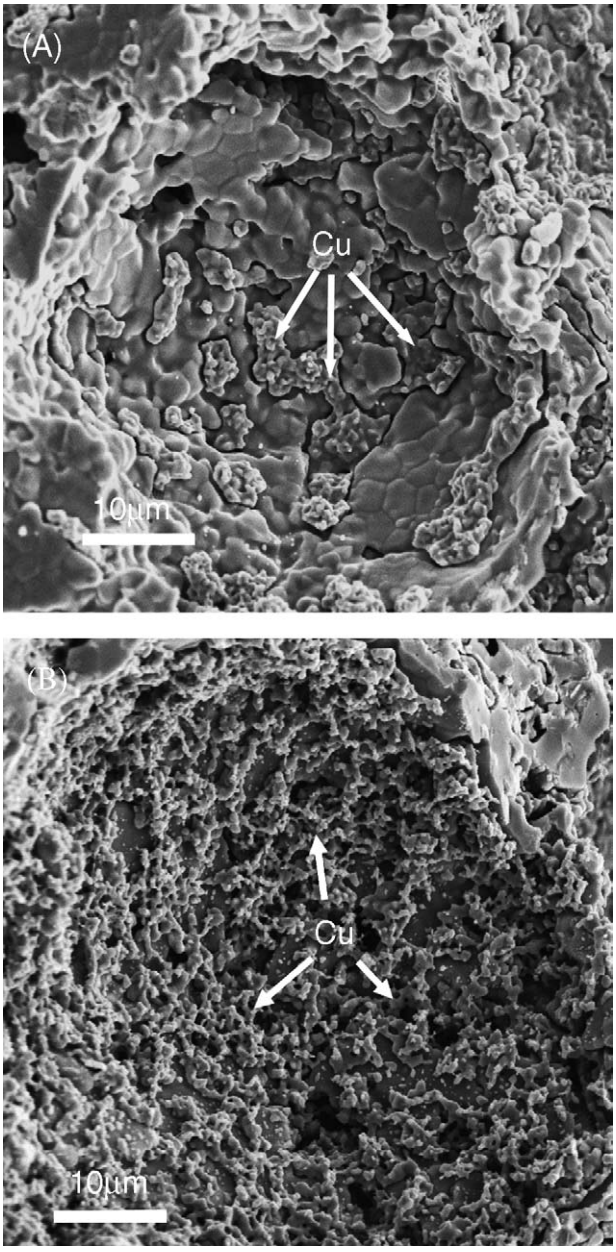

Fig. 2. SEM images of porous YSZ blocks after impregnation of CeO_2 and Cu (13 vol% Cu and 5 vol% CeO_2) and subsequent reduction in H_2 for 2 h at 973 K. The Cu was added using the (A) nitrate-only and (B) nitrate/urea methods.

contain 13 vol% Cu and 5 vol% CeO_2. Unlike ceria, which forms a film on the surface of the YSZ [15], the Cu deposits are readily apparent in each micrograph. These images show dramatic differences in the morphology of the Cu deposits produced by the two different impregnation methods. Impregnation using only aqueous copper nitrate produced relatively large patches of copper agglomerates, while a much more continuous Cu layer was produced when urea was added to the impregnation solution. When impregnating with the copper nitrate solution, the deposition procedure proceeds via precipitation of $Cu(NO_3)_2$ during evaporation of the water. The size and shape of the Cu deposits therefore depend on the size of the water droplets during drying and, as shown in Fig. 2A, results in relatively large Cu particles. In contrast, when urea is used, homogenous nucleation of $Cu(OH)_2$ occurs upon heating to 350 K and as shown in Fig. 2B, this gives a more even Cu distribution.

While the images in Fig. 2 show the initial morphology of the Cu deposits, it is likely that some sintering of the Cu will occur during operation of a fuel cell, especially at temperatures in excess of 973 K [16]. In order to investigate this possibility, SEM images were collected after annealing the samples used in Fig. 2 for 2 h in H_2 at 1173 K. Fig. 3 dis-

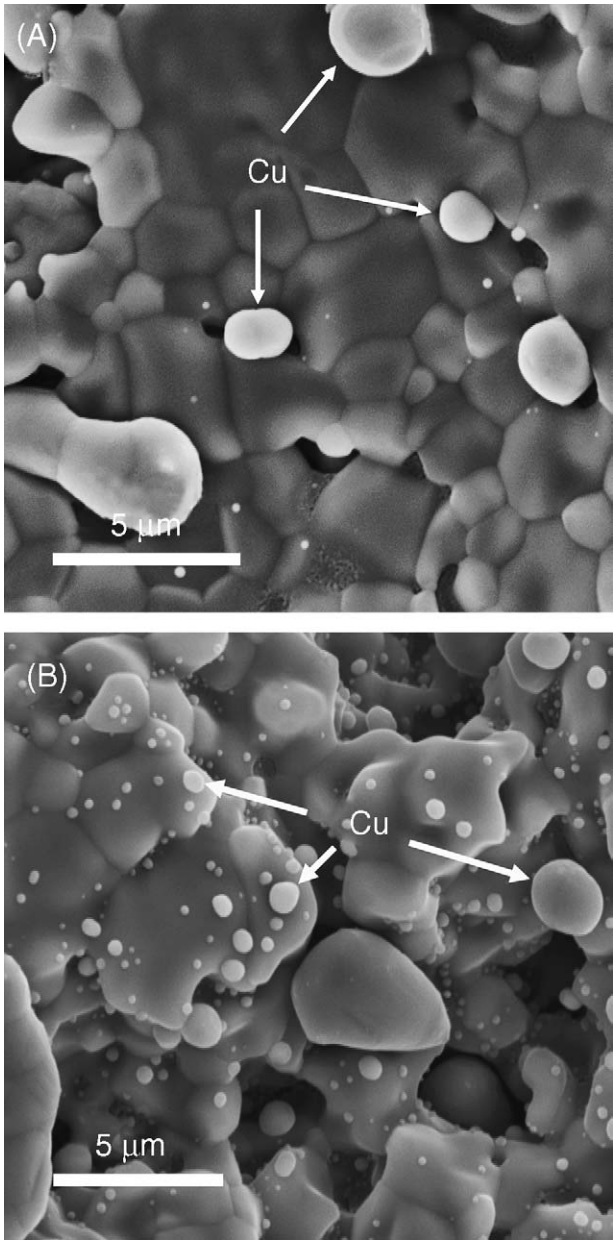

Fig. 3. SEM images obtained near the center of Cu/CeO_2/YSZ samples (13 vol% Cu and 5 vol% CeO_2) that were heated in H_2 at 1173 K for 2 h. The Cu was added using the (A) nitrate-only and (B) nitrate/urea methods.

plays higher resolution SEM images of the surface of a large pore near the center of each of the H_2-annealed samples. For the sample impregnated without adding urea the SEM image in Fig. 3A shows sintering of the Cu deposits has occurred resulting in the formation of isolated spherical Cu particles ~2 μm in diameter. Fig. 3B which displays the corresponding image for the sample impregnated using urea shows a similar result. The Cu film has again undergone significant agglomeration producing isolated Cu particles, which in this case range in size from 1–3 μm. One needs to be careful when interpreting the SEM images since they provide insight only into the structure of the Cu deposits in the large macropores formed by the PMMA pore formers. The morphology of the Cu films in the smaller pores may be different. Due to the confined geometry, the sintering of the Cu in the smaller pores is also likely to be less severe than that in the large macropores. With these caveats in mind, the SEM images still suggest that in both cases upon annealing in H_2 at 1173 K the Cu layer sinters and tends to become less continuous.

The images in Fig. 3 show that for both deposition methods after annealing at 1173 K the Cu layer consists of isolated Cu particles. Based on this observation one might expect the annealed samples to exhibit relatively low bulk electronic conductivities. This is indeed the case for the sample impregnated with Cu using urea. Increasing the annealing temperature from 973 to 1173 K caused the conductivity to decrease by more than 80%. In contrast, for the sample impregnated with Cu using only the nitrate solution, increasing the annealing temperature to 1173 K caused only a modest 12% decrease in conductivity. There are several possible explanations for this apparent inconsistency between the conductivity and SEM data for this sample. As noted above, the SEM image only shows the morphology of the Cu in the large macropores and it is likely that the structure is somewhat different in the smaller pores. More importantly, the impregnation of $Cu(NO_3)_2$ without urea results in the enrichment of Cu near the surface of the YSZ block due to capillary forces bringing the salt solution to the surface of the porous matrix during the drying process. Therefore, the conductivity measured using surface attached electrodes may not be representative of that in the center of the block.

Demonstration of the surface enrichment of Cu in the absence of urea is given by the SEM results presented in Fig. 4. Fig. 4A shows a higher resolution SEM image taken near the exposed surface of the YSZ block impregnated with Cu using the nitrate-only method after annealing to 973 K in H_2. This image contains a much higher concentration of Cu than that in the image near the center of the block shown in Fig. 2A. The Cu also appears to be in the form of a well-connected porous film. In contrast, the image taken near the surface of the sample impregnated with Cu using urea shown in Fig. 4B is similar to that obtained near the center of the block and contains isolated Cu particles with a relatively wide size distribution. These results suggest that the nitrate-only impregnation method does not produce a homogeneous distribution of Cu in the porous YSZ block and there is Cu enrichment

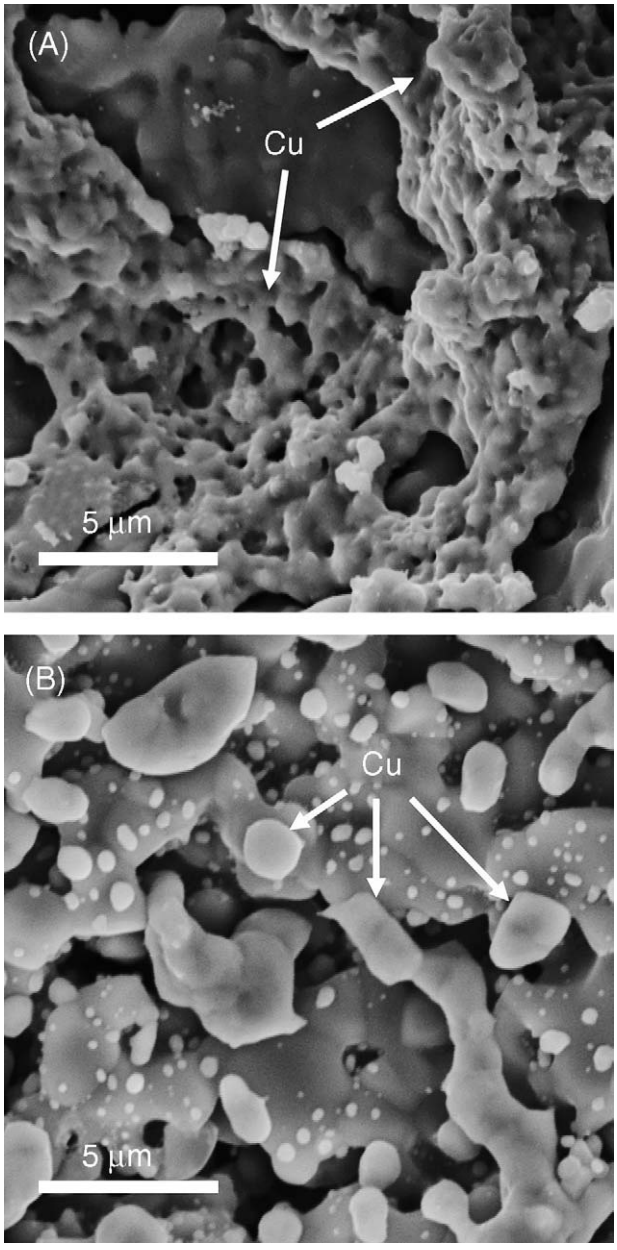

Fig. 4. SEM images obtained near the surface of Cu/CeO_2/YSZ samples (13 vol% Cu and 5 vol% CeO_2) that were heated in H_2 at 1173 K for 2 h. The Cu was added using the (A) nitrate-only and (B) nitrate/urea methods.

near the surface. They also account for the trends in the electronic conductivity as a function of annealing temperature for samples impregnated with and without the addition of urea.

3.3. Fuel cell measurements

The conductivity and microscopy results provide considerable insight into the structure and distribution of the Cu layer as a function of the impregnation method. In order to understand how the Cu distribution influences anode performance, the performance of a series of SOFCs with impregnated anodes while operating on H_2 was measured. As was

the case for the conductivity measurements, the effect on performance of varying the maximum temperature to which the fuel cell was exposed, was evaluated.

Fig. 5A shows voltage and power density versus current density curves measured at 973 K for a nitrate-only cell with an anode containing 16 vol% Cu and 12 vol% CeO_2 while operating on humidified H_2 (3% H_2O). The anode for this cell was impregnated with Cu using the nitrate-only method. Impedance spectra measured at a current density of 300 mA cm^{-2} are also presented as Cole–Cole plots in part (B) of the figure. The *V–I* curves for this cell show that the performance decreased appreciably after thermal treatments in H_2. The maximum power density for the cell was 252 mW cm^{-2} after exposure to H_2 for 2 h at 973 K and decreased to 224 mW cm^{-2} after treating for 3 h in H_2 at 1073 K, and 134 mW cm^{-2} after treating for 2 h in H_2 at 1173 K. The impedance spectra show that this decrease in performance was accompanied by an increase in the Ohmic portion of the area specific resistance (ASR) of the cell, which corresponds to the intercept of the first arc in the impedance spectrum with the real axis from 0.40 to 1.07 Ω cm^2. These results are consistent with the SEM images which show that upon heating to 1173 K the Cu film in the bulk of the anode sinters into large, isolated Cu particles. Thus, the increase in the Ohmic part of the ASR can be attributed to an increase in the resistance of the anode due to Cu sintering.

Fig. 6 displays an analogous set of data for a cell identical to that used in Fig. 5 except that the nitrate/urea method was used to impregnate the Cu into the anode. The results for this cell are nearly identical to those obtained from the cell impregnated using the nitrate-only method. The performance decreased and the Ohmic part of the cell ASR increased upon heating to 1073 and 1173 K. This can again be attributed to sintering of the Cu in the anode. Table 3 lists the maximum power density and the Ohmic part of the ASR as a function of the thermal treatment for all of the cells used in this study. The trends in the data in this table for the effect of treating at elevated temperatures in H_2 are consistent with those observed in Figs. 5 and 6.

In addition to studying how annealing in H_2 at temperatures up to 1173 K affected cell performance, the effect of exposing the 16/12 (Cu/CeO_2) cell to butane (C_4H_{10}) at 973 K was investigated. In previous studies, we have shown that the performance of Cu/CeO_2/YSZ anodes while operating

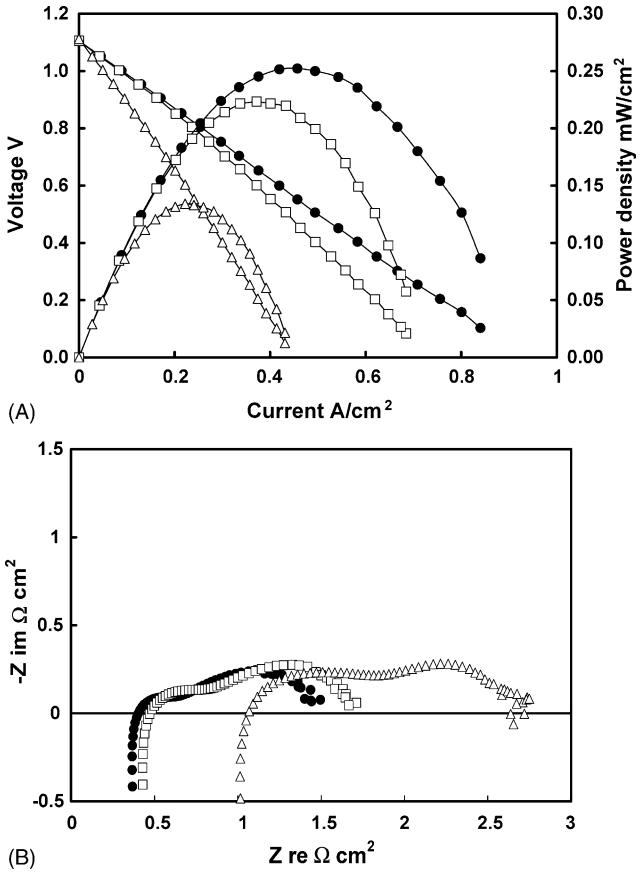

Fig. 5. (A) Voltage and power density vs. current density and (B) impedance spectra obtained at a current density of 300 mA cm^{-2} for a cell with an anode (16 vol% Cu and 12 vol% CeO_2) prepared using the nitrate-only method operating on humidified H_2 at 973 K after annealing at 973 K for 2 h (●), 1073 K for 3 h (□) and 1173 K for 2 h (△).

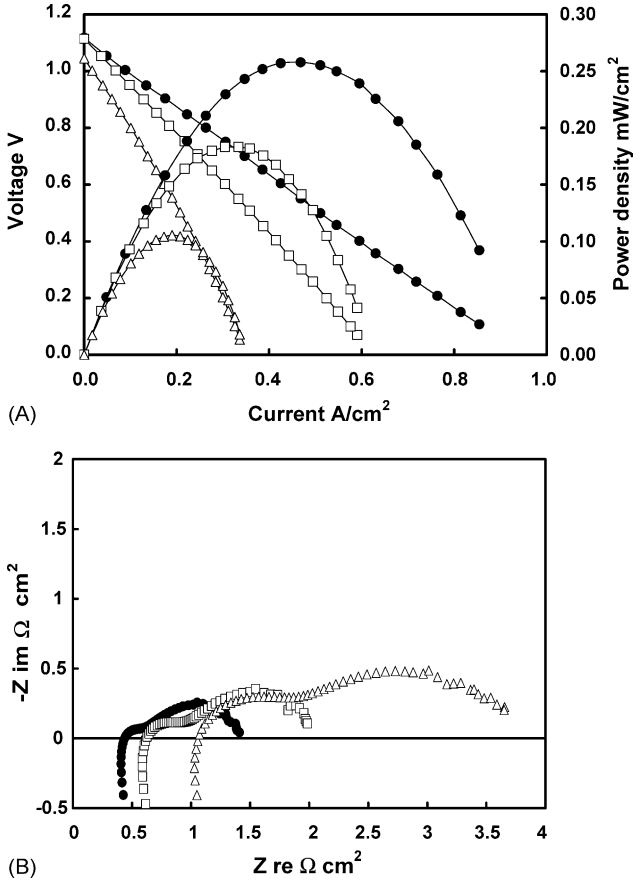

Fig. 6. (A) Voltage and power density vs. current density and (B) impedance spectra obtained at a current density of 300 mA cm^{-2} for a cell with an anode (16 vol% Cu and 12 vol% CeO_2) prepared using the nitrate/urea method operating on humidified H_2 at 973 K after annealed at 973 K for 2 h (●), 1073 K for 3 h (□) and 1173 K for 2 h (△).

Table 3
Maximum power density and Ohmic part of the ASR for cells with Cu/CeO_2/YSZ anodes fabricated using the nitrate and nitrate/urea methods

Composition (vol%)	H_2 annealing temperature (K)	Impregnated with Cu nitrate		Impregnated with Cu nitrate urea	
		Power density ($mW\,cm^{-2}$)	Ohmic part of ASR ($\Omega\,cm^2$)	Power density ($mW\,cm^{-2}$)	Ohmic part of ASR ($\Omega\,cm^2$)
5% Cu, 15% ceria	700	153	0.89	165	0.81
	1073	132	1.17	125	1.06
	1173	84	1.83	82	1.52
9% Cu, 10% ceria	700	244	0.50	238	0.40
	1073	172	0.76	169	0.56
	1173	90	1.92	78	1.23
11% Cu, 8% ceria	700	247	0.50	197	0.59
	1073	211	0.56	148	0.79
	1173	101	1.45	28	12.03
13% Cu, 5% ceria	700	247	0.45	223	0.54
	1073	178	0.64	165	0.76
	1173	64	2.30	70	2.06
16% Cu, 8% ceria	700	229	0.50	255	0.41
	1073	223	0.52	188	0.55
	1173	105	1.54	62	2.39
16% Cu, 12% ceria	700	252	0.40	258	0.43
	1073	224	0.47	183	0.62
	1173	134	1.07	105	1.06

on H_2 can in some cases be enhanced by exposure of the anode to butane [12,17]. The Cu/CeO_2 components of the anode do not catalyze the formation of carbon fibers from hydrocarbons as does the Ni component of conventional Ni/YSZ and Cu/CeO_2/YSZ anodes have been shown to exhibit stable performance while operating directly on hydrocarbon fuels [2–6,8,12,17]. When using hydrocarbon fuels, however, gas phase pyrolysis reactions that occur at temperatures above ~950 K can produce polyaromatic tars that can condense and form a film on the surface of the anode [12,18]. This tar layer is electronically conducting, relatively stable under reducing conditions and can serve to enhance the conductivity of the anode. For example, in a previous study we have shown that coating the surface of a porous YSZ block similar to that used here with a layer of polyaromatic tar by briefly exposing it to butane at 973 K caused the electronic conductivity of the YSZ block to increase from 0.002 to 0.22 $S\,cm^{-1}$. For Cu/CeO_2/YSZ anodes in which there is poor connectivity in the Cu layer we have shown that an enhancement in performance while operating on H_2 that occurs following exposure of the cell to butane is due to the increased conductivity provided by the deposited tar layer. In the present study, several of the cells were exposed to butane under maximum current conditions at 973 K in order to coat the exposed surfaces with a thin layer of the conducting polyaromatic tar. This allowed us to introduce a continuous layer within the anode that had a relatively low electronic conductivity. For cells with anodes with a high Cu loadings and dispersion the addition of the conducting tar layer would not be expected to significantly affect performance while operating on H_2. For cells with anodes with low Cu loadings or poor connectivity in the Cu layer, however, the tar film would be expected to provide conduction paths between isolated Cu particles, thus enhancing both the anode conductivity and the cell performance while operating on H_2. Since the tar layer has a much lower conductivity than Cu, the extent of the performance enhancement following tar deposition provides a qualitative measure of the Cu dispersion within the anode.

The butane exposure experiments were conducted for the two cells with an anode composition of 16 vol% Cu and 12 vol% CeO_2, one synthesized using the nitrate method and one synthesized using the nitrate/urea method. The anode of each cell was exposed to dry butane at 973 K after the anode had been heated in H_2 at 1173 K. Periodically, the fuel was switched back to H_2 in order to measure the cell performance. For the cell with the anode fabricated using the nitrate-only method, it was observed that the performance on H_2 recovered to levels close to that obtained for the cell prior to heating it to 1173 K. For this cell after a 3 h exposure to butane, the maximum power density for humidified H_2 fuel at 973 K was 275 $mW\,cm^{-2}$, which is slightly higher than that obtained from the cell initially. In contrast, for the cell with the anode fabricated using the nitrate/urea method, exposure to butane resulted in a much smaller recovery of the cell performance. For this cell, very little recovery of the performance was observed after exposure to butane for 3 h. Longer butane exposure did produce some recovery and after 6 h in butane the maximum power density when operating on H_2 at 973 K was 147 $mW\,cm^{-2}$, which is still 40% less than that obtained from the fresh cell prior to heating to 1173 K.

The spatial distribution of Cu is the most significant difference in the structure of the anodes produced by the

two different impregnation methods. As discussed above, the nitrate-only method resulted in a higher concentration of Cu in the near surface region compared to the nitrate/urea method. The SEM images show that even after heating to 1173 K in H_2 the nitrate-only anodes contain a continuous Cu film near the surface. The results obtained from the cells that had been heated to 1173 K in H_2 and then exposed to butane suggest that this Cu film plays an important role in current collection. For the cells used in this study, the current collector on the anode consisted of an Au wire ring approximately two-thirds the diameter of the cell that was attached to the surface of anode using an Au paste. For the cell with the anode impregnated with Cu using the nitrate-only method, the continuous Cu film in the near surface region of the anode, in effect, acts as part of the external current collector. For this cell after sintering the Cu at 1173 K, deposition of the tar-like film upon exposure to butane caused complete recovery of the cell performance. This result demonstrates that the tar-like film sufficiently enhanced the conductivity within the anode such that conduction in the out-of-plane direction, i.e. from the three-phase boundary to the Cu film near the surface of the anode, did not limit cell performance. Since there was not a Cu film on the surface of the anode for the nitrate/urea-impregnated cell, the external current collector for this cell was composed entirely of the Au wire ring. Thus, for this cell, both high in-plane and out-of-plane conduction within the anode is required in order to obtain good performance. The incomplete recovery of the performance of this cell following carbon deposition suggests that the enhancement of the anode conductivity by the carbon film was insufficient to provide a low resistance conduction path over the longer length scales required for this anode.

In order to test this hypothesis, experiments were performed using two cells in which a tar-like film formed by exposure to butane at high temperature was used exclusively to provide electronic conduction within the anode. The anodes in these cells were impregnated with 5 vol% CeO_2 and no Cu. The external current collector for one of the cells was identical to that used in the other cells in this study and consisted of an Au wire ring that was attached using Au paste. The current collect for the second cell consisted of a gold mesh attached using an Au paste that covered the entire surface of the anode. The anodes in these cells were activated by exposing them to flowing butane at 973 K. The cell performance was then measured at 973 K in flowing H_2. As shown in Fig. 7, the maximum power for the cell with the Au mesh current collector was 210 mW cm^{-2} after exposure to butane for only 30 min. This power density is only slightly less than that obtained from similar cells in which Cu was also added to the anode. In contrast, the maximum power for the cell with the Au wire current collector was only 150 mW cm^{-2}, even after exposure to butane for 3 h. These results are consistent with the arguments presented above and indicate that the relatively low-conductivity, carbonaceous film produced by exposure to butane provides an adequate conduction path

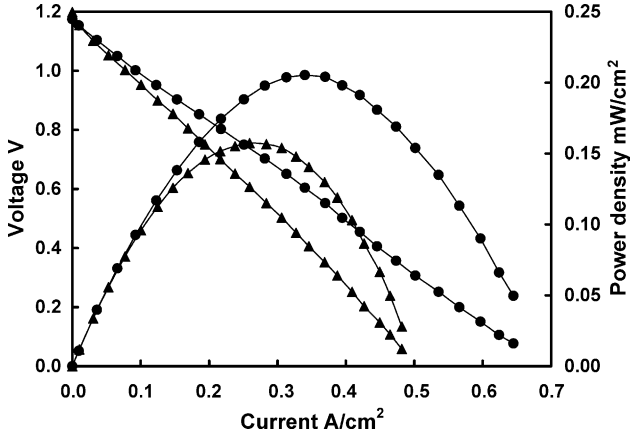

Fig. 7. Voltage and power density vs. current density for a cell with an anode containing only CeO_2 operating on humidified H_2 at 973 K. An (●) Au mesh and (▲) an Au wire ring were used as the external current collectors on the anode. The data were collected after exposing the anode to butane at 973 K.

across the thickness of the anode, but limits cell performance when conduction over longer lengths scales, such as those in the lateral direction, are required.

Finally, another interesting observation form this study is how the cell performance correlates with the Ohmic ASR of the cell. Fig. 8 displays a plot of maximum power at 973 K when using H_2 as the fuel as a function of the inverse of the overall cell Ohmic ASR, given by the high-frequency intercept of the first arc in the Cole–Cole plot of the cell impedance spectrum with the real axis, for a series of cells. These cells all had identical YSZ electrolyte layers and LSM cathodes, but had Cu/CeO_2 impregnated anodes that contained a range of concentrations of Cu and CeO_2 and were subjected to various heat treatments in order to vary the extent of the sintering of the Cu layer. Thus, the primary difference between the cells is the Ohmic resistance of the anode which is reflected in a change in the Ohmic portion of the cell ASR. Note that the plot is nearly linear. For cells with linear *V–I* curves, a plot

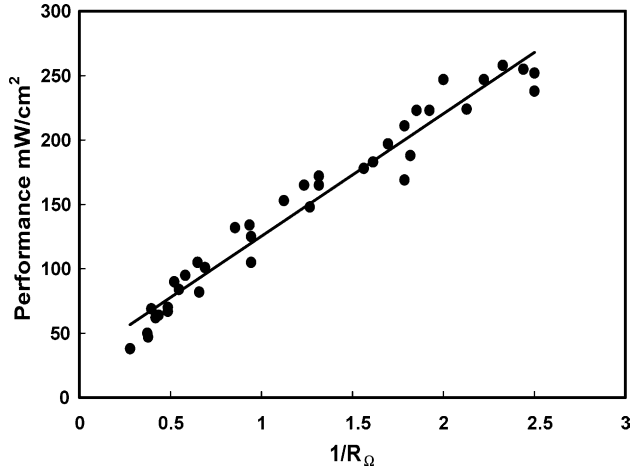

Fig. 8. Maximum power density vs. the inverse of the Ohmic part of the ASR for a series of cells with Cu/CeO_2/YSZ anodes operating on humidified H_2 at 973 K.

of the maximum power density as a function of the inverse of total ASR of the cell should be linear. The fact that in this case a linear correlation is also observed when using only the Ohmic portion of the ASR is somewhat surprising since it implies that the total cell ASR is proportional to the Ohmic portion of the ASR, which in general should not be the case. One possible explanation for this result is that the conductivity of the impregnated anodes used in this study also provides a measure of the active surface area at the three-phase boundary. If this is the case, an increase in the Ohmic resistance of the anode produced by sintering of the Cu layer would lead to proportional increases in the ASR of the other components in the cell.

4. Conclusions

The results of this study show that the addition of Cu to a porous YSZ block via impregnation and subsequent drying of aqueous copper nitrate solutions produces an inhomogeneous distribution of the Cu. SEM and conductivity measurements show that for this impregnation method there is a higher concentration of Cu near the surface of the YSZ block relative to that in the bulk. In contrast, Cu impregnation using aqueous copper nitrate solutions plus urea produced a more homogenous metal distribution throughout the porous YSZ block.

$Cu/CeO_2/YSZ$ anodes fabricated using both the nitrate and nitrate/urea methods for copper deposition exhibit good performance when operating on humidified H_2 at 973 K. Performance degradation was observed, however, upon annealing the impregnated anodes to 1073 and 1173 K in H_2 due to agglomeration of Cu layer and the formation of isolated Cu particles.

Acknowledgements

The authors gratefully acknowledge financial support from the U.S. Office of Naval Research and from Franklin Fuel Cells.

References

[1] M. Boaro, J.M. Vohs, R.J. Gorte, J. Am. Ceram. Soc. 86 (2003) 395.
[2] R.J. Gorte, S. Park, J.M. Vohs, C.H. Wang, Adv. Mater. 12 (2000) 1465.
[3] R.J. Gorte, J.M. Vohs, J. Catal. 216 (2003) 477.
[4] R.J. Gorte, J.M. Vohs, S. McIntosh, Solid State Ionics 175 (2004) 1.
[5] S. Park, R. Craciun, J.M. Vohs, RJ. Gorte, J. Electrochem. Soc. 146 (1999) 3603.
[6] S. Park, R.J. Gorte, J.M. Vohs, Appl. Catal. A Gen. 200 (2000) 55.
[7] S. Park, R.J. Gorte, J.M. Vohs, J. Electrochem. Soc. 148 (2001) A443.
[8] J.M. Vohs, S. Park, R.J. Gorte, Nature 404 (2000) 265.
[9] S. McIntosh, J.M. Vohs, R.J. Gorte, Electrochim. Acta 47 (2002) 3815.
[10] T. Shishido, Y. Yamamoto, H. Morioka, K. Takaki, K. Takehira, Appl. Catal. A Gen. 263 (2004) 249.
[11] G.J. de A.A. Soler-Illia, R.J. Candal, A.E. Regazzoni, M.A. Blesa, Chem. Mater. 9 (1997) 184.
[12] S. McIntosh, H. He, S.I. Lee, O. Costa-Nunes, V.V. Krishnan, J.M. Vohs, R.J. Gorte, J. Electrochem. Soc. 151 (2004) A604.
[13] D.W. Dees, T.D. Claar, T.E. Easler, D.C. Fee, F.C. Mrazek, J. Electrochem. Soc. 134 (1987) 2141.
[14] P. Holtappels, N. Kiratzis, C.E. Hatchwell, M. Mogensen, J.T.S. Irvine, Fuel Cells 1 (2001) 211.
[15] H. He, J.M. Vohs, R.J. Gorte, J. Electrochem. Soc. 150 (2003) A1470.
[16] M.S. Spencer, M.V. Twigg, Appl. Catal. A Gen. 212 (2001) 161.
[17] S. McIntosh, J.M. Vohs, R.J. Gorte, J. Electrochem. Soc. 150 (2003) A470.
[18] C.Y. Sheng, A.M. Dean, J. Phys. Chem. A 108 (2004) 3772.